

Microstructural investigation of the oxidation behavior of Cu in Ag-coated Cu films using a focused ion beam transmission electron microscopy technique

This content has been downloaded from IOPscience. Please scroll down to see the full text.

2016 Jpn. J. Appl. Phys. 55 06JG01

(<http://iopscience.iop.org/1347-4065/55/6S3/06JG01>)

View [the table of contents for this issue](#), or go to the [journal homepage](#) for more

Download details:

IP Address: 121.163.25.5

This content was downloaded on 26/07/2016 at 02:44

Please note that [terms and conditions apply](#).



Microstructural investigation of the oxidation behavior of Cu in Ag-coated Cu films using a focused ion beam transmission electron microscopy technique

Ji Hwan Kim and Jong-Hyun Lee*

Department of Materials Science and Engineering, Seoul National University of Science and Technology, Seoul 139-743, Republic of Korea

*E-mail: pljh@snut.ac.kr

Received October 6, 2015; accepted January 12, 2016; published online May 18, 2016

With the aim of elucidating a detailed mechanism for the oxidation behavior in submicron Cu particles coated with a thin Ag layer, the dewetting of Ag and the oxidation behavior of Cu in Ag-coated Cu films upon heating were investigated with a focused ion beam transmission electron microscopy technique. A slight dewetting of the Ag layer began at approximately 200 °C and aggregates of Cu₂O particles were formed on the Ag layer, indicating that the initial Cu₂O phase was formed on the thin Ag layer. Voids were formed in the Cu layer because of Cu atoms diffusing through the thin Ag layer to be oxidized in the upper Cu₂O aggregates. After being heated to 250 °C, the Ag layer became more irregular, and in some regions, it disappeared because of intensive dewetting. The number and average size of the voids also increased. At 300 °C, a hollow structure with a Cu₂O shell was formed. Pillar-like structures of unoxidized Cu and large voids were found under the Cu₂O layer.

© 2016 The Japan Society of Applied Physics

1. Introduction

With the advantages of facile processing techniques and low processing temperatures, electrically conductive adhesives (ECAs) have been identified as indispensable assembly materials in the electronic packaging industry and are widely used in the manufacturing of microelectronics.¹⁻⁴ Typical ECAs are composed of a resin formulation and an electrically conductive metal filler; the filler is conventionally Ag powder because Ag has excellent intrinsic electrical and antioxidation properties. In addition, the electrical properties of contacts between Ag fillers are excellent because AgO₂ is also conductive when its surface is oxidized.³ Ag powder is also used as a filler in conductive pastes for the printing of electrodes and line contacts.⁵⁻¹⁰ Such printing processes can eliminate the complicated steps of lithographic processes and are compatible with the rapidly growing printed electronics industry and roll-to-roll manufacturing.⁸⁻¹⁰

However, both industrial and academic researchers have investigated alternatives to Ag-based fillers to increase the competitiveness and widen the range of low-cost ECA and conductive paste applications. As a result, Ag-coated Cu fillers have been widely investigated as the first alternative.¹¹⁻²³ In such filler materials, Cu, which has an electrical conductivity that is similar to that of Ag,^{24,25} is used as a low-cost core material and the Ag coating functions as an antioxidation layer and a contact surface.

The applicability of Ag-coated Cu fillers to curing temperatures below 200 °C has been reported in the literature. Zhang et al.¹³ reduced the electrical resistivity of untreated, Ag-coated, Cu flakes from 1.3×10^{-3} to 2.4×10^{-4} Ω·cm by using a flake filler that was surface-treated with an amine-based silane coupling agent. Nishikawa et al.¹⁴ reported an electrical resistivity of approximately 1.5×10^{-4} Ω·cm when Ag-coated Cu spheres with a diameter of 5 μm were used, which shows the importance of the surface condition and morphology of the filler metal. In addition, Ag-coated Cu fillers of submicron size have also been recently studied to improve the performance improvement of ECAs or the preparation of ECAs with an ability of fine patterning.^{15,17,19,22} The range submicron filler applications is expected to grow constantly.



Fig. 1. (Color online) Schematic illustration showing the cross section of the Ag-coated Cu film.

Despite the successful application of Ag-coated Cu particles as a filler material, it has also been reported that the oxidation of Ag-coated Cu particles abruptly begins at temperatures above 200 °C because of the dewetting of the Ag coating and the formation of nodule-type Ag agglomerates on the Cu surface.^{20-22,26-28} This is due to the phase separation, caused by the positive enthalpy of mixing (104 meV/atom at 50 at. % of Cu),²⁹ a small difference (0.03) in electronegativity,³⁰ a large lattice mismatch (12%),^{31,32} and the instability of the Ag/Cu interface.³² However, the lack of research on the oxidation initiation time and scarcity of direct evidence mean that little is known about the oxidation process of Ag-coated Cu above 200 °C. Hence, we performed a transmission electron microscopy (TEM)-based study of the dewetting of a thin Ag layer and the oxidation behavior of Cu in a Ag-coated Cu fillers as functions of heating temperature. When a 15 wt % Ag layer is coated on a 500-nm-diameter Cu core particle, the thickness of the Ag layer becomes very small, approximately 10 nm.

2. Experimental methods

Figure 1 shows a schematic diagram of the cross section of a Ag-coated Cu film. The Cu layer was sputtered onto a Ti adhesion layer (thickness, ≈10 nm), which was formed on a 10 × 10 cm² Si wafer. The average thickness of the Cu layer was approximately 100 nm. After preparing the Cu layer, immersion Ag plating was implemented through the galvanic displacement reactions that occur between Ag ions and Cu atoms when the Cu-coated wafer is dipped into a bath solution. Before the plating procedure, the etching and

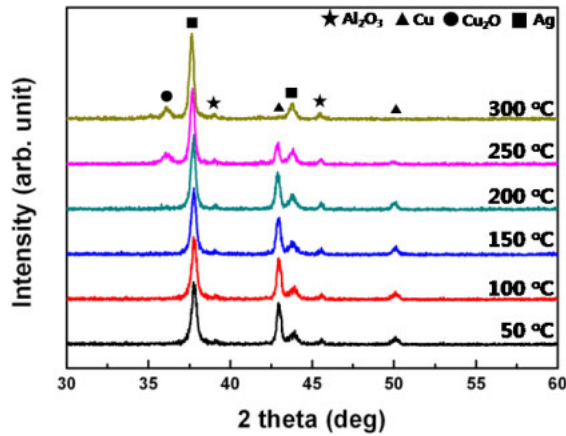


Fig. 2. (Color online) XRD pattern of the Ag-coated Cu film as a function of temperature (50–300 °C).³³⁾

rinsing of the sample were conducted for 1 min using a 1 : 9 v/v mixture of sulfuric acid (H₂SO₄, 99.9%, Ducksan Chemical, 95%, Samchun Pure Chemical) and ethanol (C₂H₅OH, 99.9%, Ducksan Chemical), and deionized water, respectively. The composition of the plating bath was as follows. Diethylene glycol [DEG, (HOCH₂CH₂)₂O, 99%, Sigma-Aldrich] was selected as the solvent, and silver nitrate (AgNO₃, 99.9%, Kojima Chemicals) and citric acid [HOC(COOH)(CH₂COOH)₂, >99.5%, Sigma-Aldrich] were used as the Ag-ion source and complexing agent, respectively. All chemicals were used without further processing or purification. To prepare the plating bath solution, 0.1 g of AgNO₃ and 1 g of citric acid were dissolved in 100 ml of DEG, and then the solution was mixed. During the plating process, the mixed solution was continuously stirred with a magnetic stirrer at 300 rpm. The bath temperature was fixed at 40 °C. After 30 min of immersion, the Ag-coated Cu film was rinsed with ethanol and deionized water for 1 min to remove any impurities. The average thickness of the Ag coating was approximately 10 nm. The Ag-coated Cu film was then dried for 24 h at room temperature.

To investigate the oxidation behavior of the Cu layer as a function of temperature under air atmosphere, the Ag-coated Cu film was heated on a hot plate to 300 °C in steps of 50 °C. The heating rate was fixed at 5 °C/min and the holding time at each temperature was 5 min. After the holding time, phase analysis was conducted with in situ X-ray diffraction (XRD; Philips X'pert MPD). The cross section of the Ag-coated Cu film was investigated by TEM (FEI Tecnai 20). The TEM samples were prepared with a dual-beam focused ion beam (FIB; FEI Quanta 200 3D) setup. Energy-dispersive spectroscopy (EDS) analysis was also performed to provide information on which elements are present in specific parts and on the relative quantity of each element.

3. Results and discussion

Figure 2 shows the XRD pattern of the Ag-coated Cu film as a function of temperature (50–300 °C) under air atmosphere (the Al₂O₃ phase does not need to be considered because the signal is from the specimen holder).³³⁾ Up to 200 °C, the XRD patterns do not show any marked changes. However, as the temperature increases to 250 °C, the intensity of the Cu phase decreases considerably and that of the Cu oxide (Cu₂O)

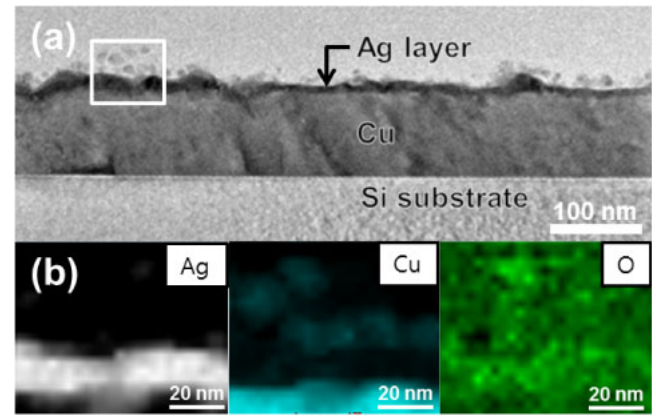


Fig. 3. (Color online) (a) Cross-sectional TEM image and (b) elemental mapping images of the Ag-coated Cu film heated to 200 °C.

phase abruptly increases. On the other hand, the intensity of the Ag phase is unchanged by the increase in temperature to 250 °C. Therefore, these results indicate that the rapid oxidation of the Cu layer occurs as the temperature increases from 200 to 250 °C.

Figures 3(a) and 3(b) show a cross-sectional TEM image and elemental mapping images, of the Ag-coated Cu film heated to 200 °C respectively. The elemental mapping images [Fig. 3(b)] were acquired in the region indicated by the white box in Fig. 3(a). The microstructure of the Ag-coated Cu film [Fig. 3(a)] is very similar to that observed before the sample was heated, except for the increased roughness on the plated Ag layer. However, there are many aggregates of tiny particles on top of the Ag layer. The elemental mapping of these aggregates shows that Cu is present, but the mapping image for O is noisy.

Figure 4(a) shows an enlarged cross-sectional TEM image of the top surface, while Fig. 4(b) shows the elements detected by EDS at the highlighted points in Fig. 4(a). The microstructure of the top surface appears to resemble the shape of the aggregated particles, and Cu and O are the major elements detected at point 1. Ag is the dominant element at point 2, which is between the top surface and the initially sputtered Cu layer (point 3). Thus, the phase of the aggregated particles found above the thin Ag layer was indexed as Cu₂O. The formation of the initial Cu₂O phase was observed on the thin Ag layer, which is contrary to the studies indicating that the oxidation process is initiated in the exposed Cu regions after the complete dewetting of the Ag layer.^{20,21,26)} Although Hai et al. reported a 260-nm-thick Ag layer on a 5 μm Cu particle,²⁰⁾ Tsai et al. and Grouchko et al. reported Ag layers of 2.5 and <2 nm, respectively.^{21,26)} Although the difference in thickness was large, no study reported that the initial Cu₂O phase was formed on a thin Ag layer. Hai et al.'s study was performed only at the microscale by SEM.²⁰⁾ Thus, detailed observations such as the formation of the initial Cu₂O phase were lacking. Although the TEM image of Ag-coated Cu particles before Ag dewetting was presented in the other studies, the dewetting images were obtained by SEM or a detailed oxidation mechanism was not presented.^{21,26)} The results in Fig. 4 imply that Cu atoms diffuse from the initial Cu layer through the thin Ag layer and form aggregates that are several nanometers in size. The extremely high surface energy of Ag (890 × 10⁻³ N/m)

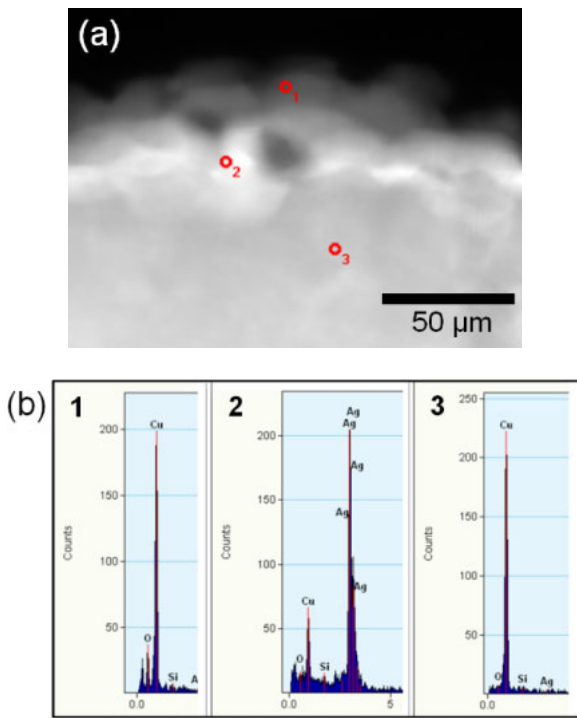


Fig. 4. (Color online) (a) Enlarged TEM image of the top surface of the Ag-coated Cu film heated to 200 °C and (b) the elements detected by EDS at the highlighted points in (a).

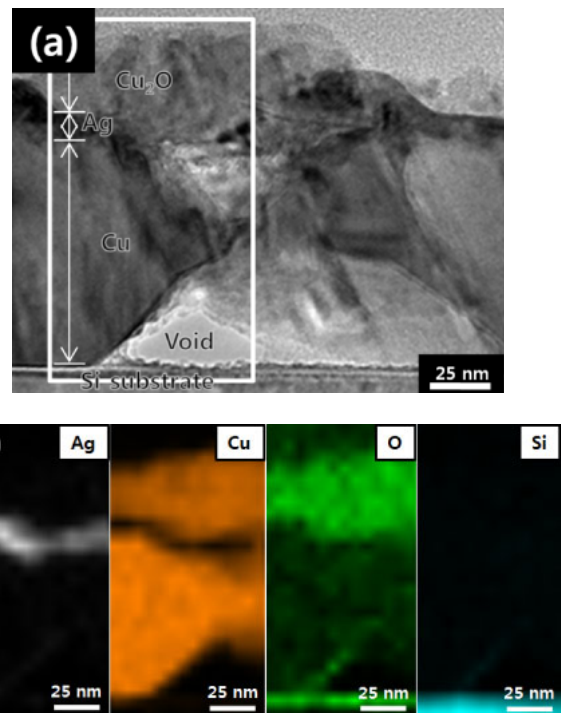


Fig. 5. (Color online) (a) Cross-sectional TEM image of the Ag-coated Cu film heated to 200 °C and (b) elemental mapping images of the region indicated by the white box in (a).

compared with that of Cu_2O is considered to be the driving force for the diffusion of Cu atoms.^{34,35} After diffusing to the surface, the tiny particles, which have an extremely large surface area, are then promptly oxidized and form aggregates. The dewetting behavior of the Ag layer was mild because of the relatively low temperatures involved and the advantage of being deposited on a flat surface as opposed to the curved surfaces of particles. However, because of the slight dewetting of Ag, peaks and troughs are present in the Ag layer covering the Cu film, as shown in Fig. 3(a). Hence, the troughs can be considered fast diffusion channels for the Cu atoms. These results indicate that the dewetting of Ag in the Ag-coated Cu film is initiated when the temperature reaches approximately 200 °C, which also begins the initial stages of oxidation in the Cu layer.

The intensive outward diffusion of Cu atoms and further oxidation were observed in another Cu layer of the same sample, as shown in Fig. 5. As a result of the diffusion of Cu through the thin Ag layer, both Cu and O are clearly observed above the Ag layer, indicating that the phase above the Ag layer is Cu_2O . A few voids are also observed in the upper and lower regions of the sputtered Cu layer; these voids are formed by the depletion of Cu via the aforementioned diffusion (the voids were filled with polymer-based contaminants during the FIB machining of the sample). It has been reported that the intense oxidation of a Cu particle or Ag-coated Cu particle creates a vacant core because the oxidation occurs at the air/ Cu_2O interface, not at the Cu_2O /Cu interface.^{20,36} After the initial formation of Cu_2O in this sample, the Cu atoms from the initial Cu layer then continuously diffuse through the thin Ag layer to react with O_2 in air. The formation of voids appears to be linked to the grain boundaries in the initial Cu layer, which implies that the fastest Cu diffusion channels are the grain boundaries.

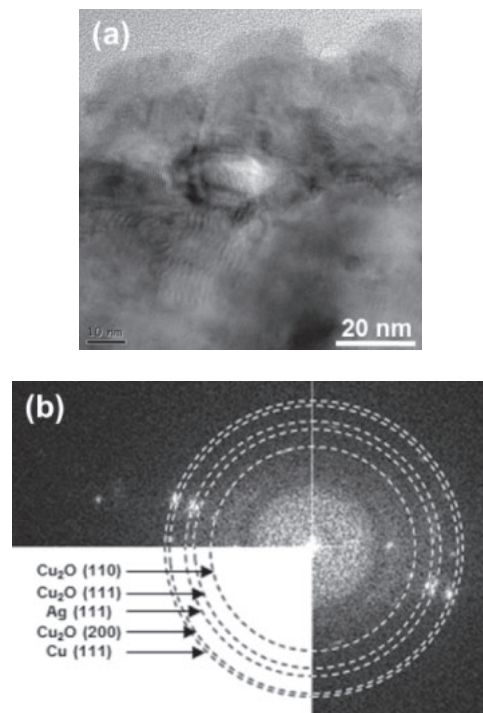


Fig. 6. (a) High-resolution TEM image and (b) FFT pattern of the Ag-coated Cu film heated to 200 °C.

Figure 6 shows a high-resolution TEM image and a fast Fourier transform (FFT) pattern of a Ag-coated Cu film heated to 200 °C. The FFT pattern indicates that there is a Cu_2O phase next to the Ag and Cu phases in the layer. This result corresponds well to EDS results in Fig. 4 and elemental mapping results in Fig. 5. However, because of the low XRD resolution, the Cu_2O phase was not detected in the sample heated to 200 °C in Fig. 2.

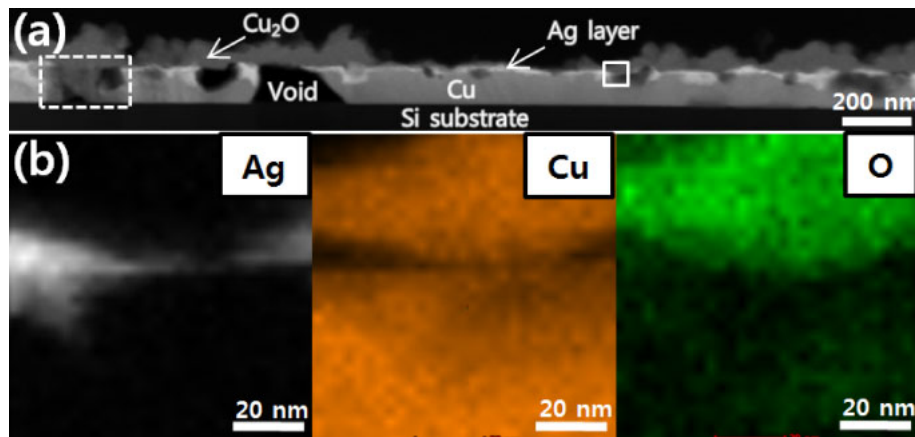


Fig. 7. (Color online) (a) Cross-sectional HAADF-TEM image and (b) elemental mapping images of the Ag-coated Cu film heated to 250 °C.

Figure 7 shows a cross-sectional, high-angle annular dark-field (HAADF)-TEM image and elemental mapping images of a Ag-coated Cu film heated to 250 °C. The HAADF-TEM image clearly shows the different phases because of the strong contrast between heavy and light elements. Hence, in Fig. 7(a), the Cu_2O phase above the irregular Ag layer is darker than the pure Cu phase below the Ag layer. The elemental mapping images [Fig. 7(b)] acquired from the square solid line in Fig. 7(a) confirm that the phase above the Ag layer is Cu_2O and that the phase below the Ag layer is pure Cu. The Ag layer is not present in some regions because of the dewetting process, and the lower parts in the regions are mostly voids. Many small and large voids are present in the sputtered Cu layer and the total volume of the voids increases rapidly after the film is heated to 250 °C, unlike the sample heated to 200 °C. Most of the voids are linked to the upper Cu_2O layer, implying that the Cu_2O phase is formed by the outward diffusion of Cu from the initial Cu layer. The direct oxidation of the sputtered Cu layer also occurs in some regions where the Ag layer is dewetted [square dotted line in Fig. 7(a)]. This is attributed to the penetration of air through narrow gaps where the upper Cu_2O phase does not exist. These results indicate that the exposure of the sputtered Cu layer to air at 250 °C induces the rapid oxidation of the layer when the Ag layer, which acts as an oxidation barrier, is removed.

A cross-sectional TEM image and an FFT pattern of an Ag-coated Cu film heated to 300 °C are shown in Fig. 8. The Ag layer splits into irregular agglomerates and finding pure Cu is difficult because most of the initial Cu is oxidized. There are a few pillar-like structures of unoxidized Cu and large voids under the Cu_2O layer because the Cu atoms in the initial Cu layer rapidly diffuse to the surface of the upper Cu_2O layer, and the resulting voids become linked to the increased temperature.

The results of this study are similar to those obtained by studies of the dewetting of Ag and the formation of hollow structures with a CuO shell in Cu–Ag core–shell particles that are heated to 500 °C.²⁰ However, in this FIB TEM study, it was found that the initial Cu_2O phase forms on the thin Ag layer at approximately 200 °C, which is contrary to the reports that claim that the oxidation of Cu is initiated in the exposed Cu areas after the complete dewetting of the Ag layer.^{20,21,26} Furthermore, the formation of hollow structures

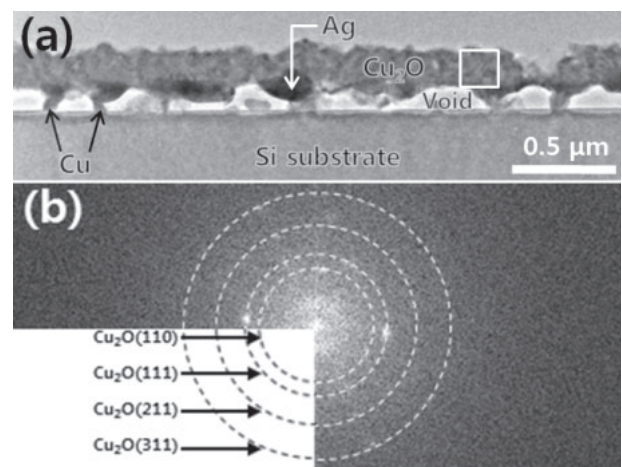


Fig. 8. (a) Cross-sectional TEM image and (b) FFT pattern of the Ag-coated Cu film heated to 300 °C.

with a Cu_2O shell was almost completed at around 300 °C, as opposed to 500 °C.²⁰

4. Conclusions

To elucidate the oxidation behavior in submicron Ag-coated Cu particles, the oxidation and phase transformation of Ag-coated Cu films fabricated by sputtering and immersion plating was investigated with a FIB TEM technique as a function of heating temperature. The initial thickness of the Ag layer was 10 nm. The slight dewetting of the Ag layer began at approximately 200 °C, and aggregates of tiny Cu_2O particles were formed in many local regions on top of the Ag layer. The observation that the initial formation of the Cu_2O phase occurred on the thin Ag layer is contrary to the studies indicating that the oxidation of Cu is initiated in the exposed Cu areas after the Ag layer is dewetted. Thus, Cu atoms in the initially sputtered Cu layer diffuse through the thin Ag layer to be oxidized in the Cu_2O aggregates. The diffusion channel for Cu atoms in the Cu layer is the grain boundaries. The thinner regions of the Ag layer, which are generated by the dewetting process, are also thought to act as channels for the fast diffusion of Cu atoms. Furthermore, because of this outward diffusion, a few voids were formed in the sputtered Cu layer. After being heated to 250 °C, the Ag layer became more irregular and disappeared in some regions because of intensive dewetting. The number and average size of the

voids also increased. Most of the voids were linked to the Cu₂O layer, further confirming that the Cu₂O phase is formed via the outward diffusion of the initial Cu layer. When the sample was heated to 300 °C, a hollow structure with a Cu₂O shell was formed. Pure Cu was hard to find because of the severe outward diffusion and oxidation of Cu. Thus, there were only a few pillar-like structures of unoxidized Cu and large voids under the Cu₂O layer.

Acknowledgments

This work was supported by the Materials and Components Technology Development Program (10047681) funded by the Ministry of Trade, Industry and Energy (MI, Korea). The authors also thank Korean Basic Science Institute (KBSI) for TEM analysis.

- 1) H. Jiang, K.-S. Moon, J. Lu, and C. P. Wong, *J. Electron. Mater.* **34**, 1432 (2005).
- 2) F. Tan, X. Qiao, J. Chen, and H. Wang, *Int. J. Adhes. Adhes.* **26**, 406 (2006).
- 3) Y. Li and C. P. Wong, *Mater. Sci. Eng. R* **51**, 1 (2006).
- 4) D. I. Tee, M. Mariatti, A. Azizan, C. H. See, and K. F. Chong, *Compos. Sci. Technol.* **67**, 2584 (2007).
- 5) M. M. Hilali, K. Nakayashiki, C. Khadilkar, R. C. Reedy, A. Rohatgi, A. Shaikh, S. Kim, and S. Sridharan, *J. Electrochem. Soc.* **153**, A5 (2006).
- 6) W. Zeng, H. Wu, C. Zhang, F. Huang, J. Peng, W. Yang, and Y. Cao, *Adv. Mater.* **19**, 810 (2007).
- 7) D.-Y. Shin, Y. Lee, and C. H. Kim, *Thin Solid Films* **517**, 6112 (2009).
- 8) F. C. Krebs, *Sol. Energy Mater. Sol. Cells* **93**, 465 (2009).
- 9) A. Hu, J. Y. Guo, H. Alarifi, G. Patane, Y. Zhou, G. Compagnini, and C. X. Xu, *Appl. Phys. Lett.* **97**, 153117 (2010).
- 10) J. Yan, G. Zou, A. Wu, J. Ren, J. Yan, A. Hu, and Y. Zhou, *Scr. Mater.* **66**, 582 (2012).
- 11) X. Xu, X. Luo, H. Zhuang, W. Li, and B. Zhang, *Mater. Lett.* **57**, 3987 (2003).
- 12) H. T. Hai, J. G. Ahn, D. J. Kim, J. R. Lee, H. S. Chung, and C. O. Kim, *Surf. Coatings Technol.* **201**, 3788 (2006).
- 13) R. Zhang, W. Lin, K. Lawrence, and C. P. Wong, *Int. J. Adhes. Adhes.* **30**, 403 (2010).
- 14) H. Nishikawa, S. Mikami, K. Miyake, A. Aoki, and T. Takemoto, *Mater. Trans.* **51**, 1785 (2010).
- 15) D. S. Jung, H. M. Lee, Y. C. Kang, and S. B. Park, *J. Colloid Interface Sci.* **364**, 574 (2011).
- 16) J. Zhao, D. Zhang, and J. Zhao, *J. Solid State Chem.* **184**, 2339 (2011).
- 17) Y. Peng, C. Yang, K. Chen, S. R. Popuri, C.-H. Lee, and B.-S. Tang, *Appl. Surf. Sci.* **263**, 38 (2012).
- 18) X. G. Cao and H. Y. Zhang, *Powder Technol.* **226**, 53 (2012).
- 19) S. J. Kim, E. A. Stach, and C. A. Handwerker, *Appl. Phys. Lett.* **96**, 144101 (2010).
- 20) H. T. Hai, H. Takamura, and J. Koike, *J. Alloys Compd.* **564**, 71 (2013).
- 21) C.-H. Tsai, S.-Y. Chen, J.-M. Song, I.-G. Chen, and H.-Y. Lee, *Corros. Sci.* **74**, 123 (2013).
- 22) C. K. Kim, G.-J. Lee, M. K. Lee, and C. K. Rhee, *Powder Technol.* **263**, 1 (2014).
- 23) H.-W. Cui, J.-T. Jiu, T. Sugahara, S. Nagao, K. Sugauma, and H. Uchida, *Electron. Mater. Lett.* **11**, 315 (2015).
- 24) S. Jeong, S. H. Lee, Y. Jo, S. S. Lee, Y.-H. Seo, B. W. Ahn, G. Kim, G.-E. Jang, J.-U. Park, B.-H. Ryu, and Y. Choi, *J. Mater. Chem. C* **1**, 2704 (2013).
- 25) W. Li, M. Chen, J. Wei, W. Li, and C. You, *J. Nanopart. Res.* **15**, 1949 (2013).
- 26) M. Grouchko, A. Kamysny, and S. Magdassi, *J. Mater. Chem.* **19**, 3057 (2009).
- 27) A. Muzikansky, P. Nanikashvili, J. Grinblat, and D. Zitoun, *J. Phys. Chem. C* **117**, 3093 (2013).
- 28) S.-S. Chee and J.-H. Lee, *J. Mater. Chem. C* **2**, 5372 (2014).
- 29) C. Wolverton, V. Ozoliņš, and A. Zunger, *Phys. Rev. B* **57**, 4332 (1998).
- 30) L. Pauling, *The Nature of the Chemical Bond* (Cornell University Press, New York, 1960) 3rd ed., p. 93.
- 31) C. Kittel, *Introduction to Solid State Physics* (Wiley, New York, 1976) 5th ed., p. 32.
- 32) D. Bochicchio and R. Ferrando, *Phys. Rev. B* **87**, 165435 (2013).
- 33) J. H. Kim, Y. H. Cho, and J.-H. Lee, *J. Microelectron. Packag. Soc.* **21** [2], 79 (2014).
- 34) V. A. Zhabrev, S. S. Kayalova, and L. P. Efimenko, *Glass Phys. Chem.* **31**, 606 (2005).
- 35) P. Sebo, B. Gallois, and C. H. P. Lupis, *Metall. Trans. B* **8**, 691 (1977).
- 36) M. Tsuji, S. Hikino, R. Tanabe, M. Matsunaga, and Y. Sano, *CrystEngComm* **12**, 3900 (2010).